

Absolute silicon molar mass measurements, the Avogadro constant and the redefinition of the kilogram

This content has been downloaded from IOPscience. Please scroll down to see the full text.

2014 Metrologia 51 361

(<http://iopscience.iop.org/0026-1394/51/5/361>)

View [the table of contents for this issue](#), or go to the [journal homepage](#) for more

Download details:

IP Address: 194.117.40.96

This content was downloaded on 22/09/2015 at 10:14

Please note that [terms and conditions apply](#).

Absolute silicon molar mass measurements, the Avogadro constant and the redefinition of the kilogram

R D Vocke Jr, S A Rabb and G C Turk

National Institute of Standards and Technology, 100 Bureau Drive, Gaithersburg, MD 20899, USA

E-mail: vocke@nist.gov

Received 25 February 2014, revised 3 May 2014

Accepted for publication 6 May 2014


Published 25 June 2014

Abstract

The results of an absolute silicon molar mass determination of two independent sets of samples from the highly ^{28}Si -enriched crystal (AVO28) produced by the International Avogadro Coordination are presented and compared with results published by the Physikalisch-Technische Bundesanstalt (PTB, Germany), the National Research Council (NRC, Canada) and the National Metrology Institute of Japan (NMIJ, Japan). This study developed and describes significant changes to the published protocols for producing absolute silicon isotope ratios. The measurements were made at very high resolution on a multi-collector inductively coupled plasma mass spectrometer using tetramethylammonium hydroxide (TMAH) to dissolve and dilute all samples. The various changes in the measurement protocol and the use of TMAH resulted in significant improvements to the silicon isotope ratio precision over previously reported measurements and in particular, the robustness of the $^{29}\text{Si}/^{30}\text{Si}$ ratio of the AVO28 material. These new results suggest that a limited isotopic variability is present in the AVO28 material. The presence of this variability is at present singular and therefore its significance is not well understood. Fortunately, its magnitude is small enough so as to have an insignificant effect on the overall uncertainty of an Avogadro constant derived from the average molar mass of all four AVO28 silicon samples measured in this study. The NIST results confirm the AVO28 molar mass values reported by PTB and NMIJ and confirm that the virtual element–isotope dilution mass spectrometry approach to calibrated absolute isotope ratio measurements developed by PTB is capable of very high precision as well as accuracy. The Avogadro constant N_{A} and derived Planck constant h based on these measurements, together with their associated standard uncertainties, are $6.022\,140\,76(19) \times 10^{23} \text{ mol}^{-1}$ and $6.626\,070\,17(21) \times 10^{-34} \text{ J s}$, respectively.

Keywords: Avogadro constant, absolute silicon molar mass, multi-collector inductively coupled plasma mass spectrometer, virtual element–isotope dilution mass spectrometry, Si-28 enriched single crystal, International Avogadro Coordination, kilogram redefinition

(Some figures may appear in colour only in the online journal)

 Online supplementary data available from stacks.iop.org/Met/51/361/mmedia

1. Introduction

The molar mass measurements reported here are part of an international effort to redefine the kilogram (kg) and the mole (mol) in terms of fundamental constants of nature [1, 2]. The kilogram remains the only base unit of the International System of Units (SI) defined by a 90% Pt–10% Ir alloy cylinder,

a material artefact called the international prototype of the kilogram (IPK). The IPK was sanctioned as the unit of mass by the 1st General Conference on Weights and Measures (CGPM) late in the 19th century (1889). The IPK is kept in a vault at the International Bureau of Weights and Measures (BIPM), Sèvres, France, just outside Paris and has been used on three occasions since its adoption as the SI unit of mass.

The kilogram is a critical base unit in the SI not only because the definitions of the base units ampere, mole and candela are linked to it, but also because a number of SI derived units depend on it. These include the unit of force (newton, N), pressure (pascal, Pa), energy (joule, J) and power (watt, W). If the mass of the IPK were to change, not only would the magnitude of the unit of mass change, but the magnitudes of the aforementioned units would also change proportionately, a clearly unacceptable state of affairs in the 21st century. Thus, a redefinition of the kg from the IPK to one based on an exact value of a fundamental constant that can be readily realized in the laboratory using modern measurement techniques is long overdue.

The current plan is to redefine the kilogram in terms of an exact, fixed value of the Planck constant h [2]. At present, there are two promising independent techniques for determining h , each requiring significant metrological rigor of comparable complexity but of quite different methodology. The first approach measures h directly. It is based on an apparatus called a watt balance (WB) [3, 4] in which the power necessary to support a mass is measured both electrically in terms of voltage and resistance using the low temperature, condensed-matter quantum phenomena known as the Josephson effect and the quantum Hall effect and mechanically in terms of known standards of mass, length and time.

The second approach, called the x-ray crystal density (XRCD) method, determines h indirectly. It measures the Avogadro constant N_A by estimating the number of silicon atoms in a mole of silicon [5] from which h can be derived. In practice, the measurement of N_A is achieved by using two highly pure and polished 1 kg single crystal Si spheres, designated S5 and S8. These silicon spheres were made from a boule of isotopically enriched Si (0.999 96 ^{28}Si amount-of-substance fraction) that is also nearly crystallographically and spherically perfect [6]. By determining the mass, volume, lattice parameter of the unit cell and the molar mass of each sphere, the Avogadro constant N_A can be determined. The molar mass of the silicon in the different spheres is calculated by measuring the absolute isotopic composition of the silicon and multiplying the resulting amount-of-substance fractions by the well-known relative atomic masses $A_r(^{28}\text{Si})$, $A_r(^{29}\text{Si})$ and $A_r(^{30}\text{Si})$ [7] of the three naturally occurring silicon isotopes.

The effort to determine N_A with the smallest possible relative standard uncertainty (about 2 parts in 10^8) has been underway for about four decades and has involved many different laboratories throughout the world. During the last decade, this effort has been organized and coordinated by the International Avogadro Coordination (IAC) under the auspices of the International Committee for Weights and Measures (CIPM). The effort involves not only highly precise and accurate measurements of the above mentioned quantities, but also careful characterization of the surface properties of the spheres. It should also be recognized that while the mass, volume, and surface properties of each sphere can be measured using the spheres themselves, the lattice spacing, isotopic composition (and hence molar mass), impurity content, and possible presence of any inhomogeneities can only be determined using samples taken from the vicinity of

the spheres. All materials originated from the very high-purity silicon single crystal boule made from artificially enriched ^{28}Si called AVO28 [8].

The two approaches to the determination of h discussed above, while independent, are completely comparable. This is because the product $N_A h$, called the molar Planck constant with the SI unit J s mol^{-1} , is related to other well-known constants through the relation $N_A h = c A_r(e) \alpha^2 M_u / 2 R_\infty$. Here c is the exactly known speed of light in vacuum, M_u is the exactly known molar mass constant, $A_r(e)$ is the relative atomic mass of the electron, α is the fine-structure constant, and R_∞ is the Rydberg constant. The current relative standard uncertainty of all the constants on the right-hand side of this equation is 7 parts in 10^{10} [9, 10]. This uncertainty is sufficiently small compared with the current relative uncertainties of the WB and XRCD determinations of h and N_A that each can be obtained from the other with negligible additional uncertainty. Thus, this relationship provides a rigorous check on the metrological comparability of the values and uncertainties assigned to h and N_A by the two different approaches. The goal, therefore, is to have the product of these two independently measured constants agree with the molar Planck constant $N_A h = 3.990\,312\,7176(28) \times 10^{-10} \text{ J s mol}^{-1}$ [9, 10], within a specified uncertainty.

This paper reports molar mass measurements of the AVO28 material carried out at NIST. These measurements are part of the IAC effort and the samples of AVO28 and calibration materials were provided to NIST by the IAC through the Physikalisch-Technische Bundesanstalt (PTB), Braunschweig, Germany.

1.1. Previous work

Five independent measurements of the absolute molar mass of AVO28 material have been published as part of an IAC-coordinated multi-national effort. The PTB [11], the National Research Council [12] (NRC, Ottawa, Canada) and the National Metrology Institute of Japan [13] (NMIJ, Tsukuba, Japan) have used the ‘virtual element’ isotope dilution mass spectrometry (VE-IDMS) approach developed at PTB [14–16] to produce calibrated Si molar mass measurements using commercially available multi-collector inductively coupled plasma mass spectrometers (MC ICP-MS). The two other published mass measurements of AVO28 were a calibrated traditional gas isotope ratio measurement [17] made at the Institute for Reference Materials and Measurements (IRMM), Geel, Belgium and an uncalibrated proof-of-principle secondary ion mass spectrometry time-of-flight measurement [18] made at the Institute for Physics of Microstructures, Russian Academy of Sciences.

An in-depth study [17] compared these last two measurements with the VE-IDMS results from PTB and concluded that, because of the effects of significant natural Si contamination in the first case and the lack of calibration in the second, only VE-IDMS results were sufficiently reliable and metrologically rigorous enough to provide robust molar mass values for the AVO28 material. Despite this very positive endorsement, the VE-IDMS approach to absolute Si

Table 1. Published results for the AVO28 molar mass and the Avogadro constant [5, 12, 13]. AVO28-S5 and AVO28-S8 refer to samples proximate to spheres S5 and S8, respectively. The uncertainties in parentheses are one standard uncertainty and apply to the last two significant digits.

NMI ^(a)	Method ^(b)	Molar mass (g mol ⁻¹)	Avogadro constant (mol ⁻¹)
NMIJ	MC ICP-MS	AVO28-S5: 27.976 970 07(15)	6.022 140 80(20) × 10 ²³
	VE-IDMS	AVO28-S8: 27.976 970 11(14)	
	Average:	27.976 970 09(14)	
PTB	MC ICP-MS	AVO28-S5: 27.976 970 26(22)	6.022 140 78(18) × 10 ²³
	VE-IDMS	AVO28-S8: 27.976 970 29(23)	
	Average:	27.976 970 27(23)	
NRC	MC ICPMS	AVO28-S5: 27.976 968 34(21)	6.022 140 40(19) × 10 ²³
	VE-IDMS	AVO28-S8: 27.976 968 44(27)	
	Average:	27.976 968 39(24)	

^a NMI: National Metrology Institute; NMIJ: National Metrology Institute of Japan; PTB: Physikalisch-Technische Bundesanstalt (Germany); NRC: National Research Council (Canada).

^b MC ICP-MS: multi-collector inductively coupled plasma–mass spectrometer; VE-IDMS: ‘virtual element’–isotope dilution mass spectrometry.

molar mass determinations has remained a very difficult and challenging measurement process. This is exacerbated by the extreme range in relative Si isotopic abundances of the AVO28 material itself, the necessity of serially measuring enriched spikes of all three Si isotopes and the ubiquity of natural Si as a possible contaminant.

The results of the three published VE-IDMS molar mass measurements of the AVO28 material [11–13] are listed in table 1 with their standard uncertainties. The value and standard uncertainty of each result are the combination of multiple measurements on different silicon chips selected from around the two silicon spheres, S5 and S8. While the standard uncertainties of the individual measurements are quite similar ($\approx 8 \times 10^{-9}$, relative), the difference in the averages of the NRC and the PTB–NMIJ molar mass determinations is nearly 10 times larger.

Table 1 also lists the published values and uncertainties for the Avogadro constants calculated by combining these molar masses with the published density and unit cell measurements for spheres S5 and S8 [19]. The effect of the aforementioned discrepancy is demagnified because the molar mass contributes less than 5% to the increased overall uncertainty of the derived Avogadro constants.

For these results to be useful, the contributing measurements must achieve metrological compatibility for their derived constants. The *International Vocabulary of Basic and General Terms in Metrology* (VIM) [20] defines metrological compatibility as:

‘the property of a set of measurement results for a specified measurand, such that the absolute value of the difference of any pair of measured quantity values from two different measurement results is smaller than some chosen multiple of the standard measurement uncertainty of that difference.’

Metrological compatibility results when two or more sets of measurements, representing the same measurand, agree within a specified uncertainty. This exacting interpretation of agreement means that any results for the molar mass of AVO28 that fall outside these bounds imply that either the AVO28 material itself has significant variability in its Si isotopic

abundances, or that one or more of the measurements are biased or that one or more of the measurements have an under-assessed measurement uncertainty.

The desirability of metrological agreement between the different measurements for defining the Planck constant h underpinning the new kg definition is of sufficient importance that it is a specific recommendation of the Consultative Committee for Mass and Related Quantities (CCM) of the CIPM during the 12th Meeting of the CCM in March, 2010. While the VE-IDMS measurements described in this paper are similar to those reported by PTB, NRC and NMIJ, the approach and methodology of the NIST measurements differ in significant details and shed light on possible measurement issues that may have given rise to the observed differences in the PTB–NMIJ and NRC molar mass results (see table 1).

2. Experimental details

The overall experimental design for sample handling, dissolution and general chemistry, as well as the measurement, acquisition and reduction of data largely parallels the procedures laid out by PTB [14–16] and the later refinements by the NRC [12]. However, significant changes to the chemistry and measurement protocols were instituted to guard against potential biases arising due to sample characteristics and the challenging set of measurements necessary to detect and calibrate the absolute molar mass of the AVO28 material. Tables 2a and 2b outline the major chemical and instrumental procedures used to make these measurements¹.

2.1. Sample descriptions

All samples used in this study were produced by the IAC and distributed by the PTB. Samples from the ²⁸Si-enriched Avogadro boule are designated by the prefix AVO28. Samples

¹ Certain commercial equipment, instruments, or materials are identified in this paper in order to specify the experimental procedure adequately. Such identification is not intended to imply recommendation or endorsement by the National Institute of Standards and Technology, nor is it intended to imply that the materials or equipment identified are necessarily the best available for the purpose.

Table 2a. Summary of the key chemical procedures used by NIST in determining the absolute Si isotopic measurements of the AVO28 samples.

Chemistry	
Solvent and diluent	TMAH ^a
AVO28 ^b , AVO28-IDMS ^b solutions $w(\text{Si})$, $w(\text{TMAH})$: analyte mass fractions ^c	$w(\text{Si})$: 550 $\mu\text{g/g}^c$, 50 $\mu\text{g/g}^c$ $w(\text{TMAH})$: 6 mg/g^c
K -factor solutions ^d $w(\text{Si})$, $w(\text{TMAH})$: analyte mass fractions ^c	$w(\text{Si})$: 4 $\mu\text{g/g}^c$ $w(\text{TMAH})$: 6 mg/g^c

^a TMAH: Tetramethylammonium hydroxide ($\text{N}(\text{CH}_3)_4^+\text{OH}^-$).

^b AVO28, AVO28-IDMS: These are solutions containing the ^{28}Si -enriched material produced and distributed by the IAC. These include the AVO28 material itself and the AVO28-IDMS blends, a mix of the ^{30}Si spike and AVO28 sample.

^c Mass fraction units: $\mu\text{g/g}$ or micrograms of analyte per gram sample (10^{-6} : 1), mg/g or milligrams of analyte per gram sample (10^{-3} : 1). Note that all solution mass fractions were adjusted so that both the mass fractions of Si ($w(\text{Si})$) and the diluent ($w(\text{TMAH})$) were accurately known and controlled. The mass fraction of TMAH was held constant in all solutions.

^d K -factor solutions: These are used to determine the correction or calibration factors for the mass spectrometric silicon isotope ratio measurements (e.g. $K_{30/29} = R_{\text{True}}^{30/29} / R_{\text{Meas}}^{30/29}$ and $K_{28/29} = R_{\text{True}}^{28/29} / R_{\text{Meas}}^{28/29}$). The calibration materials include solutions made from the natural Si material WASO as well as the enriched ^{29}Si and ^{30}Si spikes and blends of these materials. The K -factors are used to correct measured $^{30}\text{Si}/^{29}\text{Si}$ and $^{28}\text{Si}/^{29}\text{Si}$ ratios to absolute ratios.

proximate to spheres S5 and S8 are identified by the numeric prefixes 5 and 8. Two independent pairs of AVO28 samples (table 3) were analysed. A pair consists of two silicon chips, one each proximate to spheres S5 and S8. The pairs have been designated with the suffixes P1 and P2 (pair 1, pair 2). AVO28 sample masses averaged approximately 200 mg.

The calibration materials used to correct the AVO28 Si isotope measurement biases (K -factor approach, see table 2b) were procured and also distributed by the PTB. They consisted of two separate sets of ^{29}Si -enriched (Si29), ^{30}Si -enriched (Si30) and natural (WASO) high-purity silicon chips. Two independent calibration sets (table 3) were created and are designated with the suffixes C1 or C2 (calibration 1, calibration 2). Table 3 identifies the different samples, describes them and gives their nominal masses. The Si29 and Si30 chip masses were around 50 mg, while the WASO chips were around 60 mg.

2.2. Chemistry

The most significant change in the NIST approach to these measurements, when compared to that taken by the PTB and NRC, involved switching the Si chemistry from a NaOH-based system to one based on tetramethylammonium hydroxide (TMAH, $\text{N}(\text{CH}_3)_4^+\text{OH}^-$). TMAH was used for sample dissolution, dilution and as a cleaning agent to effectively reduce the Si memory-effects coming from the walls of the sample uptake-tubing, nebulizers and spray chamber surfaces. NMIJ also adopted the NIST TMAH Si chemistry approach for their measurements [13].

TMAH is commonly used in the semi-conductor industry as a silicon etchant and is available as a high-purity solvent. It is quite effective in dissolving silicon chips without any discernible isotopic fractionation. It also does not significantly suppress the Si^+ signal in an inductively coupled plasma ion source, in marked contrast to Si solutions with NaOH [12]. This increased sensitivity allows one to make Si isotopic measurements with significantly less concentrated Si

solutions without compromising the need for high resolution and adequate signal intensity.

A cleaning solution of 10% (mass fraction) TMAH, when followed by high-purity water, also ensured that any memory or carry-over between samples was minimized and that the Si blank measurements reflected natural relative isotopic abundances. The solutions necessary to produce both the K -factor corrections and the AVO28 and AVO28-IDMS blends are not typical of the sample solutions that would be analysed during a high-precision isotope ratio study. Figure 1 illustrates the seven different sample solutions that are required for a completely calibrated analysis of an AVO28 sample (see the bottom of figure 1, samples encircled by a box). Five of these solutions are necessary for calibration and two are needed for the AVO28 characterization. Beneath each solution in figure 1 is a representation of the Si isotopic spectrum of that sample.

In the course of even a calibration sequence, solutions with highly variable Si isotopic abundances must be run sequentially. A simple wash-out is often not sufficient to bring a blank solution back to stable Si-baseline levels with natural Si isotopic spectrum. This is particularly true when the different and essentially mono-nuclidic silicon spike solutions are part of the run sequence. The memory carry-over phenomenon is typically a dynamic one. It changes over time as Si is absorbed or released from surfaces depending on small changes in the solution chemistries passing through the sample introduction system. The effects of memory carry-over are also not intrinsic to the solutions being analysed but are rather a function of the order in which samples are run and their degree of enrichment in one isotope over the other. These effects are most noticeable during blank measurements, which are intended to correct sample analyses for non-sample and presumably natural Si contamination. If not controlled, these effects can also lead to significant biases in which the measured signal intensities of any minor Si isotopes within a given sample are significantly over or under-corrected due to non-natural silicon spectra in blanks.

Table 2b. Summary of the key instrumental settings and procedures used by NIST in determining the absolute Si isotopic measurements of the AVO28 materials. For an explanation of the A, B, C, etc coding of samples, see footnotes j and k.

Mass spectrometry	
Mass spectrometer:	MC ICP-MS ^a (Thermo Fisher Neptune)
AVO28 measurements:	PTB VE-IDMS approach ^b
Calibration measurements:	PTB <i>K</i> -factor approach ^c
Resolution ^d (resolving slit width)	AVO28 and AVO28-IDMS measurements: VHR-16 μm <i>K</i> -factor measurements: VHR-16 μm
Nebulizer:	ESI 50 μL min ⁻¹ PFA, pumped
2-stage spray chambers:	PEEK cyclonic + PFA Scott ^e
Torch, injector ^f :	Sapphire, sapphire
Ion detection:	Faraday cup ^g : 10 ¹¹ Ω (FAR) and secondary electron multiplier ^h (SEM)
Switching between <i>K</i> -factor, AVO28 and AVO28-IDMS samples	FAR cups and the SEM were automatically reset and optimized electronically between <i>K</i> -factor and AVO28 measurements
Run of order of <i>K</i> -factor solutions and AVO28 solutions:	<i>K</i> -factor and AVO28 samples were combined in a stratified random manner in a run. Samples from S5 ⁱ and S8 ⁱ were always run as pairs with same calibration. Randomized order of samples A, B, C, AB, BC ^j Randomized order of samples X ₅ , X ₈ , CX ₅ , CX ₈ ^k

^a MC ICP-MS—multicollector inductively coupled plasma mass spectrometer.

^b PTB VE-IDMS Approach—also called the ‘virtual element’ (VE) approach. The abundance of ²⁸Si cannot be measured directly in the AVO28 material. Therefore, the amounts of ²⁹Si and ³⁰Si in this material are treated as an impurity (*x_{imp}*) and measured by IDMS using a ³⁰Si spike. The ²⁸Si abundance in AVO28 is then derived by difference (1 - *x_{imp}*), producing absolute mole fractions of each Si isotope in the sample. This approach was conceived by and first applied by the PTB [14].

^c PTB *K*-factor Approach—biases for the mass spectrometric isotope ratio measurements are corrected using measurements made on a set of end-member solutions of enriched ²⁸Si, ²⁹Si and ³⁰Si together with gravimetrically prepared blends of those end-members [15]. This specific approach was developed by the PTB [14] for the three-isotope Si system. Only two of the calibration combinations are needed to calculate the *K*-factors.

^d Resolution—all Si measurements were made at very high resolution (*M*/*ΔM* >> 1000) due to polyatomic isobaric interferences. Resolution on the Neptune comes from the entrance slit width controlling the ion image. The High Resolution slit on a Neptune is typically 25 μm. These measurements were made with a 16 μm slit which means higher and therefore better resolution coupled with lower signal intensities. These measurements are therefore described as being made at very high resolution (VHR).

^e PEEK cyclonic, PFA Scott—types of spray chambers, used in tandem, made of the chemically inert materials PEEK (polyetheretherketone) and PFA (perfluoroalkoxy copolymer).

^f Torch, injector—the injector delivers the aerosol (in this case, Si in a matrix of TMAH) that is being analysed into an Ar plasma that is created and sustained by the torch.

^g Faraday cup—an ion detector that measures the current produced by an ion beam. This current, when passed through a high ohmic resistor, gives a voltage. All Faraday measurements were made with 10¹¹ Ω resistors.

^h SEM—an ion detector that measures the ion fluence in a beam as counts per second. All ³⁰Si signals in the AVO28 samples were measured on the axially mounted SEM that had been cross-calibrated with a Faraday detector and were corrected for coincident ions (dead-time correction).

ⁱ S5, S8 refers to samples taken near spheres 5 and 8 in this study.

^j The shorthand notation for the different calibration solutions, in parentheses, is: WASO(A), Si29 (B), Si30 (C), WASO+Si29 (AB), Si29+Si30 (BC).

^k The shorthand notation for the different AVO28 solutions, in parentheses, is: AVO28 (X₅, X₈), Si30+AVO28 (CX₅, CX₈). The subscripts 5 and 8 refer to samples taken near sphere 5 and sphere 8, respectively.

Table 3. Identification and description of the high-purity silicon materials used for the NIST molar mass measurements of the AVO28 materials. All samples with the AVO28 prefix refer to materials that came from the ²⁸Si-enriched boule produced by the IAC [8]. They have been paired and are designated sets P1 and P2. The WASO, Si29 and Si30 prefixes refer to high purity samples of natural Si, ²⁹Si-enriched and ³⁰Si-enriched silicon that are used to produce the *K*-factor solutions for measurement calibrations. They have been divided into two calibration sets, C1 and C2.

Description	Sample name	IAC sample identification	Nominal mass
Set P1: AVO28 chips from around spheres 5 and 8	AVO28-5B2 P1	Si28-10-Pr11 part 5B2.1.1.3	0.248 g
	AVO28-8A4 P1	Si28-10-Pr11 part 8A4.1.1.3	0.245 g
Set P2: AVO28 chips from around spheres 5 and 8	AVO28-5B1 P2	Si28-10-Pr11 part 5B1.1.1.1	0.219 g
	AVO28-8B1 P2	Si28-10-Pr11 part 8B1.1.1.1	0.199 g
Calibration set C1	Used to calibrate AVO28-P1 samples and to check the calibration of AVO28-P2 samples	Si29-3Pr10C ₂ F _z part 1.2.2	0.064 g
		Si30-3Pr10C ₂ F _z part 2.2.1	0.063 g
		WASO-04 41969/04/72-75 part Mi1	0.066 g
Calibration set C2	Used to calibrate AVO28-P2 samples	Si29-3Pr10C ₂ F _z part 1.2.1	0.051 g
		Si30-3Pr10C ₂ F _z part 2.2.2	0.051 g
		WASO-04 41969/04/72-75 part Mi1	0.059 g

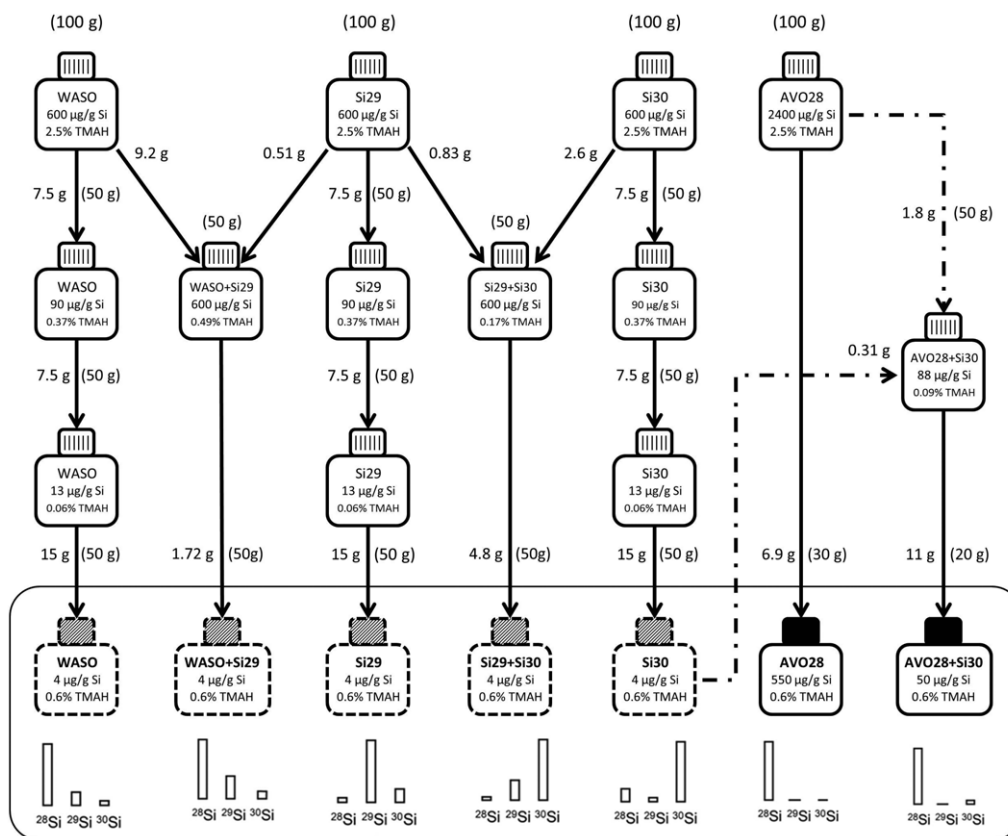


Figure 1. Generalization of the dilution scheme for the stock solutions after sample dissolution (top bottles). The solutions within the solid enclosed box at the bottom of the figure were run on the Neptune MC ICP-MS. Also shown are the mass spectra for each solution, comparing the relative intensities of their three Si stable isotopes. Samples with vertically-lined caps are the intermediate samples. Samples with dashed bottle outlines are the *K*-factor solutions while those with solid black caps are the AVO28 and AVO28-IDMS (AVO28+Spiked Si30) samples. The grams in parentheses above each bottle are the nominal target dilutions for that bottle and the non-parenthetic gram amounts are the nominal transfer amounts of the source solution. All dilutions were done gravimetrically.

The challenge of memory carry-over is typically dealt with in one of two ways. One approach is to drastically increase the intensity of all the minor isotopes in a sample analysis by increasing the total amount of silicon being analysed, thereby making even a non-normal and therefore incorrect blank correction inconsequential. Unfortunately, this approach of measuring increasingly concentrated silicon solutions also has the unintended consequence of creating higher and more non-normal blank values. These blanks then have less to do with the sample solutions that they are intended to correct and more to do with memory effects consequent from high analyte and matrix concentrations passing through the sample uptake and nebulization systems as well as the plasma chemistry. Another way to deal with this challenge is to minimize the effects of adsorption and subsequent release from tubing, spray chamber and nebulizer by keeping analyte and matrix concentrations as low as possible while using a rapid cleaning protocol that will effectively strip the analyte from any surfaces it comes into contact with. Such a memory carry-over reduction step, using 10% (mass fraction) TMAH followed by high-purity water, was integrated into the blank and sample solution measurement cycle as shown in figure 2. Adding this two-step process prior to every blank and sample measurement increased the overall per sample analysis time by nearly 6 min. Its inclusion however allowed the AVO28 and calibration samples in a complete

analysis sequence (two AVO28, two AVO28-IDMS and five calibration samples) to be run in a stratified random sample order. Stratification into AVO28 samples and calibration samples was necessary because the memory reduction after the random mixing of AVO28 and calibration samples in an analysis sequence (as manifested in blank measurements) could not be reliably controlled. This was primarily due to the extreme levels of ^{28}Si introduced by the AVO28 samples and retained in the uptake and injection systems.

2.2.1. Sample chemistry. All chemicals (HNO_3 , HF, TMAH, H_2O) used in this study were high-purity reagents. All perfluoroalkoxy alkane (PFA) bottles and containers were pre-cleaned with dilute solutions of HNO_3 and HF, rinsed with fresh 18 M Ω cm deionized (DI) H_2O and then air-dried.

The AVO28 and *K*-factor chips used to create the different sample and calibration sets were first rinsed with ethanol and acetone to remove any organics. They were then etched with a solution of 5% (volume fraction) HNO_3 + 5% (volume fraction) HF in an oven at 60 °C for 45 min to remove any surface oxidation. All sample masses were subsequently measured at NIST by the Mass and Force Group of the Physical Measurement Laboratory. The double substitution method was used to accurately determine the sample masses through a series of inter-comparisons between the sample and a standard mass.

	Sample	Analysis Method	Uptake Time	Rinse Time
Complete Si Sample Analysis Sequence	Si Memory Reduction	TMAH10 TMAH-Water Wash Method	1 min	40 s
	Blank	H2O TMAH-Water Wash Method	1 min	40 s
	Sample	BLK5 2 Isotope FAR-IC Method (50 Ratios)	2 min	40 s
		Si28A4 2 Isotope FAR-IC Method (50 Ratios)	2 min	0 s
Complete Si Sample Analysis Sequence	Si Memory Reduction	TMAH10 TMAH-Water Wash Method	1 min	40 s
	Blank	H2O TMAH-Water Wash Method	1 min	40 s
	Sample	BLK6 2 Isotope FAR-FAR Method (50 Ratios)	2 min	40 s
		bxA4 2 Isotope FAR-FAR Method (50 Ratios)	2 min	0 s

Sample	Method Analysis Cycle	Total Analysis Time
TMAH10 (10% TMAH)	4 cycles @ 30 x 0.524 s	62 s "analysis" time
H2O (DI H ₂ O)	4 cycles @ 30 x 0.524 s	62 s "analysis" time
BLKX (Blank 0.6% TMAH)	50 cycles @ 10 x 0.131 s	65 s analysis time
Si28A4 (AVO28 Sample in 0.6% TMAH)	50 cycles @ 10 x 0.131 s	65 s analysis time
bxA4 (AVO28-IDMS Sample in 0.6% TMAH)	50 cycles @ 10 x 0.131 s	65 s analysis time

Figure 2. A typical measurement protocol for an AVO28 and AVO28-IDMS sample run. The number of measurement cycles collected and the total amounts of time necessary for data collection are also listed. Note that the 10% TMAH (TMAH10) and water (H2O) steps, crucial for reducing the carry-over and memory effects of the different isotopically enriched samples that are being run sequentially, preceded each blank-sample measurement. It ensured that the measured blank solutions reflected a natural Si isotopic signature ($I(^{28}\text{Si}) \gg I(^{29}\text{Si}) > I(^{30}\text{Si})$) and allowed a stratified randomization of the sample run order. The ‘analyses’ associated with these two steps are examined only when there appears to be problems with the blank measurement that preceded each blank-sample measurement.

After weighing, each sample was placed in a PFA bottle and 10 g of 23% (mass fraction) TMAH added. The bottles, loosely capped, were heated in an oven at 60 °C for 3 to 4 days, which was sufficient for complete dissolution. The absence of any undissolved fractions was confirmed by shining a diode laser through the resultant solutions and noting the absence of light scattering.

The dissolved Si concentrate was then accurately diluted to 100 g with DI H₂O. A series of dilutions were then necessary to generate the final solutions for analysis (figure 1). The *K*-factor calibration and AVO28 solutions contained differing amounts of Si (ranging from 4 µg/g to 550 µg/g) that was dictated by the sensitivity of the MC ICP-MS at very high resolution and the abundance levels of the specific Si isotopes being measured (see figure 1). However, the TMAH matrix in all solutions was diluted to 0.6% (mass fraction) TMAH to minimize any potential mass bias effects arising from diluent concentration differences between the Si isotope ratio correction factors derived from the calibration solutions and the ratios measured in the AVO28 samples. Two completely independent sets of AVO28 samples (P1, P2) and *K*-factor calibration (C1, C2) solutions, as described in table 3, were prepared over the course of this study following the generalized dilution scheme shown in figure 1.

2.3. Mass spectrometry

All Si isotope ratio measurements were made at very high resolution on a MC ICP-MS (Neptune²) produced by

ThermoFisher Inc. The instrumental procedures used by NIST for making these measurements are summarized in table 2b. As with the chemistry, previously published approaches, described first by PTB [14–16] and later refined by NRC [12], were generally followed. Table 4 lists the general instrument and plasma settings used. There were, however, three important changes to the published procedures that directly improved the ease and quality of data acquisition.

The instrument and plasma settings as well as the Faraday cup, ion counting, zoom focus and signal processing parameters are detailed in table 4, with explanations. The most significant differences include the use of a nearly 40% smaller resolving slit (16 µm versus 25 µm) to increase the instrument’s resolution. While this smaller slit decreased the overall Si sensitivity, the ²⁹Si edge plateau on the side of the ²⁸Si¹H peak in the AVO28 and AVO28-IDMS samples was increased. Next, the dispersion lens on the Neptune was used to shift the ³⁰Si : ²⁹Si : ²⁸Si (detector positions H3 : C : L3, see table 4 for explanation of abbreviations) measurement spectrum of the *K*-factor solutions to the ³⁰Si : ²⁹Si (detector positions C : L3) measurement spectrum for the AVO28 and AVO28-IDMS samples without having to physically displace any of the detectors (table 4). This allowed separate, rapid and reproducible fine tuning of focus and measurement parameters for *K*-factor, AVO28 and AVO28-IDMS solutions. And finally, by using the dispersion lens to shift the spectrum of the AVO28 samples to the C and L3 detector positions, the SEM in the axial position of the Neptune multi-collector array could be used to measure the very low ³⁰Si signal of the AVO28

² The Neptune is an isotope ratio mass spectrometer that uses a plasma source, energy filter and magnetic sector mass filter to produce and separate beams of mono-energetic ions based on their *m/Q* ratios. The multi-collector

portion of the mass spectrometer is an array of Faraday cups and a secondary electron multiplier detector that allow ions with different *m/Q* to be detected simultaneously.

Table 4. The general MC ICP-MS plasma, Faraday (FAR) cup and SEM settings as well as the data collection parameters used in this study.

General instrument and plasma parameters				
Forward power:	1250 W			
Plasma gas flow:	16 L min ⁻¹			
Auxiliary gas flow:	0.75 L min ⁻¹			
Carrier gas flow:	1.08 L min ⁻¹			
Ni–Cu sample cone:	Used for all <i>K</i> -factor and AVO28 and AVO28-IDMS measurements			
Ni–Cu skimmer-X cone:	Used for all <i>K</i> -factor and AVO28 and AVO28-IDMS measurements			
Resolution slit:	Very high resolution (16 μm slit); used for all measurements			
Lens settings:	Tuned to give optimum Si intensity, peak shape and resolution			
Signal processing parameters				
Signal integration:	0.131 s			
Integrations; cycles; blocks:	10 integrations; 50 cycles; 1 block			
FAR amplifier and gain calibration	Three different 10 ¹¹ Ω amplifiers were used and were manually switched between the different cups every two runs. Amplifier gain calibrations were run at the start of each analysis series.			
SEM voltage, yield and cross calibration	SEM voltage: 1555 V; yield: 97.13%; cross calibrations between the SEM and FAR were run at the start of each analysis series			
Faraday cup, ion counting and zoom focus parameters				
	L3 ^a	C-fixed ^a	H3 ^a	Zoom lens
Cup positions (in mm) for <i>K</i> -factor solutions	45.650 (²⁸ Si)	FAR (²⁹ Si)	45.995 (³⁰ Si)	Focus: –3.0 V Dispersion: 0.0 V
Cup positions (in mm) for AVO28 solutions	45.650 (²⁹ Si)	SEM (³⁰ Si)	Not used	Focus: 0.6 V Dispersion: –22.4 V
Cup positions (in mm) for AVO28-IDMS solutions	45.650 (²⁹ Si)	FAR (³⁰ Si)	Not used	Focus: 0.65 V Dispersion: –21.5 V

^a The Neptune adjustable detector array is setup with a central Faraday cup (C) that is in a fixed position and therefore generally defines the high voltage-magnetic field-mass relationship for the multi-collection array. The central cup can also be electronically switched to a secondary electron multiplier (SEM) to measure very low ion currents. Additionally, there are 8 movable Faraday cups, 4 on the high mass side (H1, H2, H3 and H4) and 4 on the low mass side (L1, L2, L3, and L4) of C. L3 and H3 refer to the third movable cups on the low and high mass sides of C.

samples and then, after electronically switching back to the axial Faraday detector, to measure the ³⁰Si in the AVO28-IDMS samples (table 4).

At the start of each measurement session, the amplifier gain was calibrated and the SEM yield was measured and then cross-calibrated with the Faraday detectors. Three different 10¹¹Ω amplifiers were associated with the three Faraday cups during the course of this study. The amplifiers were switched manually between the three detectors every two analysis sessions. Signal acquisition was 10 integrations of 0.131 s duration, repeated for 50 cycles. A complete analysis sequence involving two different AVO28 and two different AVO28-IDMS sample solutions, five *K*-factor solutions, three or more check standards (SRM 990, Assay-Isotopic Standard for Silicon) as well as individual blank measurements (always preceded by the two-step memory cleaning step) took nearly 5 h. All solutions were pumped in order to maintain a constant rate of sample introduction over this time period.

Acquisition parameters were individually optimized for the various solutions to be measured and stored as discrete measurement methods. Figure 2 illustrates the sequence of steps necessary for two complete sample measurements, an AVO28 and AVO28-IDMS sample analysis and the associated individualized analysis method files. The sample run order was randomized within the AVO28 and AVO28-IDMS samples and within the *K*-factor solutions. The AVO28 solution sets were always run first to ensure that the ²⁹Si ion beam position on its

plateau, free of the ²⁸Si¹H interference, was optimum and not degraded by magnet or high voltage drift over time.

Table 5 lists the typical signals observed for the different solutions after correction for blank and background. Each detector, as well as the whole sample uptake and ionization system, experiences an extreme range in the relative mass fractions of the different Si isotopes being analysed during a complete analysis sequence. Data collected during the two-step Si memory cleaning step was used to check that the TMAH blanks had natural Si isotope spectra.

3. Results

As with the molar mass measurements reported by PTB, NMIJ and NRC, multiple AVO28 samples were analysed. Two chips were sampled near sphere S5 and two were from near sphere S8. As part of our experimental design, the AVO28-5XX and AVO28-8XX samples were always run in pairs concomitantly with a calibration solution to minimize any calibration biases in detecting differences between the 5XX and 8XX samples. These pairings are referred to in tables 3, 6, 7, 8 and 9 and figures 3, 4 and 5 as pair 1 (5B2 P1 and 8A4 P1) and pair 2 (5B1 P2 and 8B1 P2).

In addition, two independent sets of *K*-factor calibration solutions were created to test the robustness of the VE-IDMS method using TMAH. Table 3 summarizes the characteristics

Table 5. Typical signals observed for the different Si samples run during a normal analysis sequence which includes AVO28 and *K*-factor solutions. The AVO28 and AVO28-IDMS samples refer to AVO28 materials that are unspiked and spiked with Si30, respectively. The WASO, Si29 and Si30 solutions were made from natural Si, ²⁹Si-enriched and ³⁰Si-enriched silicon chips, respectively. The WASO+Si29 solution refers to a mix of WASO and Si29 while Si29+Si30 refers to a mix of Si29 and Si30. These five solutions are the basis for the *K*-factor calibrations (see figure 1). Note that all solutions have 0.6% TMAH as matrix diluent. The extremely low ²⁹Si and ³⁰Si signals in the AVO28 and AVO28-IDMS solutions necessitated an increase in the Si concentration in these samples. Note also that, due to its extreme enrichment, ²⁸Si is not measured in any of the AVO28 samples. [Si] and [TMAH] are the mean mass fractions of Si and TMAH, respectively. The letters in parentheses in the sub-title (A, AB, etc) are the shorthand designation of these respective solutions.

	TMAH blank	<i>K</i> -factor solutions					AVO28 solutions	
		WASO (A)	WASO+Si29 (AB)	Si29 (B)	Si29+Si30 (BC)	Si30 (C)	AVO28 (X)	AVO28-IDMS (CX)
[Si]	—	4 µg/g	4 µg/g	4 µg/g	4 µg/g	4 µg/g	550 µg/g	50 µg/g
[TMAH]	—	0.6%	0.6%	0.6%	0.6%	0.6%	0.6%	0.6%
²⁸ Si/ ²⁹ Si	≈13	19.7	8.99	0.0171	nm ^a	1.32	nm ^a	nm ^a
³⁰ Si/ ²⁹ Si	≈0.5	0.662	0.280	0.002 87	3.41	269	0.022	5.82
²⁸ Si (mV) ^b	≈22	9600	9110	144	60	30	nm ^a	nm ^a
²⁹ Si (mV) ^b	≈1	509	1010	10 900	2500	35	96	11
³⁰ Si (mV) ^b	≈0.5	352	335	33	7620	10 000	3 ^c	64

^a nm means not measured.

^b All intensities are representative of FAR measurements in very high resolution mode (16 µm slit) with a 10¹¹ Ω resistor and have been both blank and background corrected.

^c This ³⁰Si intensity was measured on a secondary electron multiplier, corrected and converted to equivalent mV.

of the different calibration and sample solutions. Pair 1 (AVO28-P1) was only run against calibration set C1, while pair 2 (AVO28-P2) was run against calibration sets C2 and C1.

Table 6 compares the average *K*₃₀ and *K*₂₈ corrections produced during the three sample-calibration series. The two *K*-factor corrections are complimentary within each series, correcting for approximately 5% mass bias. The differences in the specific values for the *K*-factors reflect the time integrated differences in the measurement conditions as the analyses proceeded.

As noted earlier, SRM 990, a Si isotopic reference material (iRM) with absolute Si amount-of-substance values certified in the late 1970s by NIST (then NBS), was used as a check standard. The Si amount-of-substance values of this iRM were also used to compute *K*-factors within the experimental series and they confirmed the measurements produced by the PTB approach. The details of this work are the subject of another paper comparing the effects of current instrumentation, technology and metrological approaches with those available 40 years ago.

Figure 3 summarizes the molar masses calculated for all the paired analyses used in this study. The data are divided into four groups. The AVO28-P1C1 group was the first analysed (*n* = 13) and showed that the AVO28-5B2 and AVO28-8A4 material had the same molar mass, within analytical uncertainty (figure 4 and table 7).

In an effort to mitigate the potential interference of the ²⁸Si¹H peak on the ²⁹Si peak of the AVO28 samples, purified deuterated water (²H₂O or D₂O) was used in place of normal water (¹H₂O) to dilute the TMAH, thereby shifting the ²⁸Si-hydride interference onto the ³⁰Si peak. While the two data points resulting from this measurement on the AVO28-5B2 and AVO28-8A4 materials shown in figure 3 confirm the measurements of the AVO28-P1C1 group, the Si signal in the deuterated samples was less stable. Therefore, this approach to minimizing the ²⁸Si-hydride interference was abandoned in

Table 6. Comparison of the *K*-factor measurements and their associated standard uncertainties (in parentheses) for the three sample-calibration experiment series. C1 and C2 represent the two independent calibration sets used to correct the AVO28 sample pairs P1 and P2. The P2 samples were run against both calibration solutions to confirm the slight but measurable difference in the molar masses of silicon chips AVO28-5B1 and AVO28-8B1. All calibration measurements leading to the *K*-factors were made concomitantly with their associated AVO28+AVO28-IDMS pairs. $K_{30/29} = R_{\text{True}}^{30/29} / R_{\text{Meas}}^{30/29}$, $K_{28} = R_{\text{True}}^{28/29} / R_{\text{Meas}}^{28/29}$ and *n* = the number of analyses within a series.

	<i>K</i> ₃₀	<i>K</i> ₂₈	<i>n</i>
P1C1 series	0.950 69(82)	1.0528(19)	13
P2C2 series	0.955 28(95)	1.0450(22)	13
P2C1 series	0.956 71(71)	1.0475(16)	5

favour of the very high resolution approach (table 2b). The deuterated data are presented in figure 3 only for illustrative purposes and have not been used in any of the molar mass calculations.

The AVO28-P2C2 group was the next analysed (*n* = 13). All the paired analyses suggested that the molar mass for the AVO28-5B1 material was slightly greater than the molar mass of the AVO28-8B1 material (figures 3, 4 and table 7). To confirm this difference, the same samples were run with the C1 calibration solutions. The AVO28-P2C1 group (*n* = 5) is the last series plotted in figure 3 and also reflects the same systematic difference between the AVO28-5B1 and AVO28-8B1 material observed within the AVO28-P2C2 measurements.

Figure 4 and table 7 summarize these data as average molar masses of the different analysis groupings. All data sets passed normality (Shapiro–Wilk) and equal variance (F-test) checks. Examination of the differences between and within the AVO28-P2C2 and AVO28-P2C1 measurements (Student’s *t*-test) suggest that while the differences in the means of the 5B1 P2C2 and 5B1 P2C1 measurements and the 8B1 P2C2 and 8B1 P2C1 measurements are statistically insignificant, the

Table 7. Summary of the molar mass and calculated Avogadro constants for the individual and aggregated samples analysed in this study. The uncertainties in parentheses are one standard uncertainty and apply to the last two significant digits. Unit cell, density and other parameters necessary to calculate the Avogadro constants were taken from [5, 25]. The number of samples used for the value assignment is n . The uncertainties for the combined molar masses are propagated uncertainties while the uncertainties for the combined Avogadro constants are arithmetic means.

Sample	Molar mass (mol g ⁻¹)	Avogadro constant ($\times 10^{23}$ mol ⁻¹)	n
5B2 P1C1	27.976 969 842(93)	6.022 140 86(21)	13
8A4 P1C1	27.976 969 797(90)	6.022 140 63(18)	13
Avg 5B2 P1+8A4 P1	27.976 969 820(64)	6.022 140 71(20)	
5B1 P2C2	27.976 970 12 (11)	6.022 140 92(21)	13
5B1 P2C1	27.976 970 16 (14)	6.022 140 93(21)	5
Avg 5B1 P2	27.976 970 141(71)	6.022 140 93(21)	
8B1 P2C2	27.976 969 757(92)	6.022 140 62(18)	13
8B1 P2C1	27.976 969 73 (14)	6.022 140 61(18)	5
Avg 8B1 P2	27.976 969 745(57)	6.022 140 62(18)	
Grand average	27.976 969 880(41)	6.022 140 76(19)	

Table 8. Uncertainty budget of the molar mass $M(\text{Si})$ of AVO28 chip 8B1 P2C2. The data were reduced using the revised algorithms described in [14, 21], while the uncertainties were calculated using GUM Workbench™. The relative atomic masses $M(^{28}\text{Si})$, $M(^{29}\text{Si})$ and $M(^{30}\text{Si})$ of the three silicon isotopes are taken from [7]. The uncertainties are all standard uncertainties with a coverage factor of $k = 1$.

Quantity ^a X_i	Units [X_i]	Value estimate x_i	Standard uncertainty $u(x_i)$	Sensitivity coefficient c_i	Index
$M(^{28}\text{Si})$	g/mol	27.976 926 534 694	4.4×10^{-10}	1.0	0.0%
$M(^{29}\text{Si})$	g/mol	28.976 494 664 901	5.23×10^{-10}	4.0×10^{-5}	0.0%
$M(^{30}\text{Si})$	g/mol	29.973 770 1360	2.3×10^{-8}	1.0×10^{-6}	0.0%
$R_{X\text{meas}}$	V/V	0.0281 08	1.16×10^{-4}	8.3×10^{-5}	1.1%
$R_{CX\text{meas}}$	V/V	9.2290	1.51×10^{-2}	-4.9×10^{-6}	72.5%
$R_{C\text{meas}}$	V/V	281.712	7.69×10^{-1}	3.4×10^{-9}	0.0%
$R_{C28\text{meas}}$	V/V	1.2664	2.74×10^{-2}	-7.6×10^{-9}	0.0%
$R_{B\text{meas}}$	V/V	0.003 004 26	2.97×10^{-6}	-5.5×10^{-5}	0.0%
$R_{B28\text{meas}}$	V/V	0.0163 832	2.09×10^{-5}	-4.1×10^{-5}	0.0%
$R_{A\text{meas}}$	V/V	0.692 839	4.41×10^{-4}	-1.8×10^{-6}	0.0%
$R_{A28\text{meas}}$	V/V	18.8504	1.43×10^{-2}	3.7×10^{-8}	0.0%
$R_{B\text{Cmeas}}$	V/V	3.565 46	2.36×10^{-3}	1.2×10^{-5}	9.0%
$R_{AB\text{meas}}$	V/V	0.293 447	2.08×10^{-4}	4.5×10^{-6}	0.0%
$m_{c cx}$	g	$3.541 69 \times 10^{-6}$	2.02×10^{-9}	12	7.2%
$m_{x cx}$	g	$8.792 385 \times 10^{-3}$	7.91×10^{-7}	-4.9×10^{-3}	0.2%
$m_{b bc}$	g	$4.672 15 \times 10^{-4}$	2.34×10^{-7}	8.8×10^{-2}	5.0%
$m_{c bc}$	g	$1.647 330 \times 10^{-3}$	8.24×10^{-7}	-2.5×10^{-2}	5.0%
$m_{a lab}$	g	$5.231 47 \times 10^{-3}$	2.62×10^{-6}	-1.4×10^{-4}	0.0%
$m_{b lab}$	g	$3.542 31 \times 10^{-4}$	1.77×10^{-7}	2.1×10^{-3}	0.0%
Y	[Y]	y	$u_c(y)$	$u_{rel}(y)$	
$M(\text{Si})$	g/mol	27.976 969 757	9.2×10^{-8}	3.3×10^{-9}	

^a R prefix denotes a measured ratio, m prefix denotes a mass. $R_{X\text{meas}}$: $^{30}\text{Si}/^{29}\text{Si}$ in AVO28; $R_{CX\text{meas}}$: $^{30}\text{Si}/^{29}\text{Si}$ in AVO28+Si30 (AVO28-IDMS); $R_{C\text{meas}}$: $^{30}\text{Si}/^{29}\text{Si}$ in Si30 spike; $R_{C28\text{meas}}$: $^{28}\text{Si}/^{29}\text{Si}$ in Si30 spike; $R_{B\text{meas}}$: $^{30}\text{Si}/^{29}\text{Si}$ in Si29 spike; $R_{B28\text{meas}}$: $^{28}\text{Si}/^{29}\text{Si}$ in Si29 spike; $R_{A\text{meas}}$: $^{30}\text{Si}/^{29}\text{Si}$ in WASO; $R_{A28\text{meas}}$: $^{28}\text{Si}/^{29}\text{Si}$ in WASO; $R_{BC\text{meas}}$: $^{30}\text{Si}/^{29}\text{Si}$ in blend Si29+Si30; $R_{AB\text{meas}}$: $^{30}\text{Si}/^{29}\text{Si}$ in blend WASO+Si29; $m_{c|cx}$: mass of Si30 spike in the AVO28-IDMS blend; $m_{x|cx}$: mass of AVO28 in the AVO28-IDMS blend; $m_{b|bc}$: mass of Si29 spike mixed with Si30 spike to make blend BC; $m_{c|bc}$: mass of Si30 spike mixed with Si29 to make blend BC; $m_{a|lab}$: mass of WASO mixed with Si29 spike to make blend AB; $m_{b|lab}$: mass of Si29 spike mixed with WASO to make blend AB.

difference between all 5B1 P2 ($n = 18$) and 8B1 P2 ($n = 18$) measurements is greater than would be expected by chance.

Table 8 lists a typical uncertainty budget for the molar mass calculation of a sample/calibration group, in this case AVO28-8B1 P2C2. The data were reduced using the revised algorithms given in [14, 21] and the uncertainties were calculated using those equations in GUM Workbench™ [22]. The overall uncertainty for this molar mass determination is around 3×10^{-9} , relative. It is dominated by the uncertainty in the

measurement of the AVO28-IDMS blend ($R_{CX\text{meas}} \approx 73\%$), with much lesser contributions from the Si29–Si30 calibration blend ($R_{BC\text{meas}} \approx 9\%$) and two mass measurements, Si30 spike in the AVO28-IDMS blend ($m_{c|cx} \approx 7\%$) and Si29 in the Si29 : Si30 blend ($m_{b|bc} \approx 5\%$). These four measurements control nearly 95% of the total uncertainty and demonstrate the importance of the IDMS and Si29 : Si30 blends in controlling the $^{30}\text{Si}/^{29}\text{Si}$ ratio and its correction to produce precise and accurate mole fractions of ^{28}Si , ^{29}Si and ^{30}Si in the AVO28

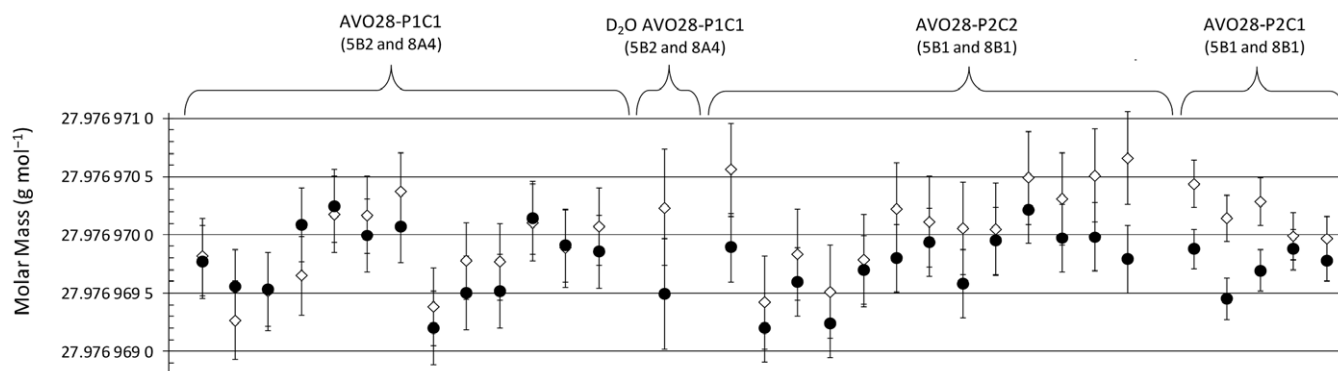


Figure 3. Summary plot of the molar masses of AVO28 samples measured in this study. AVO28-5XX (associated with sphere 5, open diamonds) and AVO28-8XX (associated with sphere 8, filled circles) samples were always measured in pairs and were therefore corrected by a common calibration set, either C1 or C2. As set out in this figure, there were four different experiments. AVO28-P1C1 means pair 1 (5B2, 8A4) corrected with calibration 1 while AVO28-P2C2 means pair 2 (5B1, 8B1) corrected with calibration 2 and so on. Data from the two deuterated measurements (D_2O AVO28-P1C1) were not included in the calculations and are only shown for reference. The uncertainties represent one standard deviation of a measurement series.

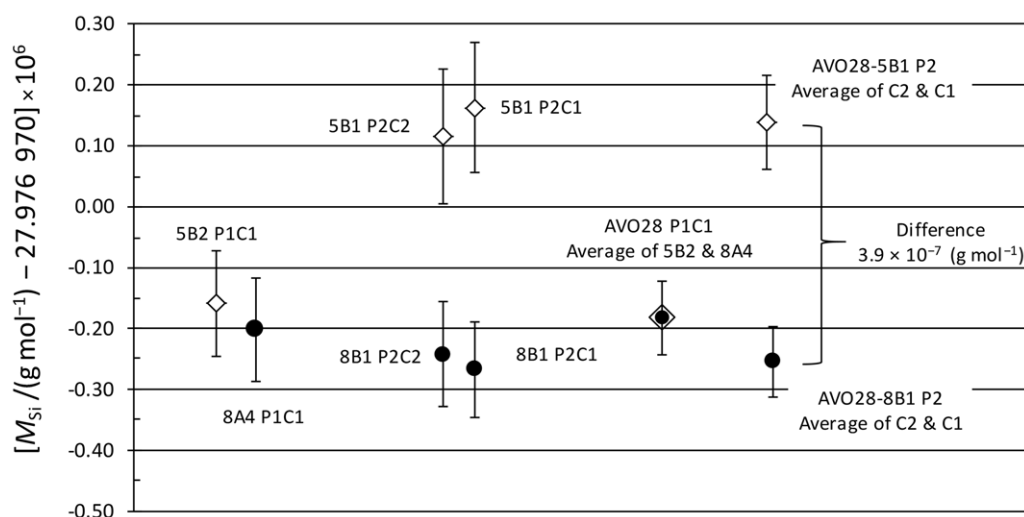


Figure 4. Summary plot of the NIST molar mass determinations on the 4 different AVO28 samples. AVO28-5XX and AVO28-8XX samples within a set were always measured in pairs (P1 or P2) and are therefore corrected by a common calibration set (C1 or C2). The values are differences at the 10^{-6} level between the measured molar masses and 27.976 970. The three different experiments summarized here were made on two independent pairs of chips taken from the vicinity of spheres S5 and S8 using two independent calibration solutions. Uncertainties are the combined standard uncertainties for the measurements on the different chip/calibration combinations.

material. The largest uncertainty components in the NRC and PTB molar mass measurement budgets were the $^{30}\text{Si}/^{29}\text{Si}$ ratio in the AVO28 material (R_X : NRC $\approx 68\%$, PTB $\approx 46\%$), followed by the transfer standard ($R_A \approx 25\%$) for NRC and the AVO28-IDMS measurement ($R_{CX} \approx 20\%$) for PTB. NMIJ's largest uncertainty component was the transfer standard ($R_A \approx 88\%$).

Figure 5 compares the absolute molar mass determinations of AVO28 materials measured by NIST, NMIJ, PTB and NRC. While the NIST, NMIJ and PTB values agree within their respective uncertainties, the NRC determination is significantly lower. Table 9 summarizes the isotopic data on the AVO28 samples measured by NIST, NMIJ, PTB and NRC. These data have been recast in terms of the different absolute $^{29}\text{Si}/^{30}\text{Si}$ ratios, which should always be greater than 1. The ratios measured in AVO28 by the different NMIs range from 32 (PTB), through 39 (NIST) to 60 (NRC). These differences

appear to be controlled by the $x(^{30}\text{Si})$ values calculated for AVO28, with the NRC reporting a ^{30}Si amount-of-substance fraction that is two times lower than that reported by NIST, NMIJ or PTB [23]. Typical values for natural Si are also provided in table 9 for comparison purposes.

Figures 6 and 7 compare the Avogadro and Planck constants derived from the different molar masses. The absolute differences between the results of the four NMIs for each of these constants are much smaller because the molar mass contributes less than a few per cent to the combined standard uncertainty of both constants. The uncertainty in the Avogadro constant is dominated by the Si sphere volume determination and this is carried over into the Planck constant uncertainty via the molar Planck constant $N_A h$ as mentioned earlier. Table 10 summarizes the values for the Avogadro and Planck constants with their associated uncertainties by NMI.

Table 9. Comparison of the absolute $^{29}\text{Si}/^{30}\text{Si}$ ratios and amount-of-substance fractions of ^{28}Si , ^{29}Si and ^{30}Si in the AVO28 samples measured by NIST (this paper), NMIJ [13]; PTB [11] and NRC [12]. Also listed are the molar masses of the virtual element (M_{VE} , the $^{29}\text{Si}+^{30}\text{Si}$ impurity) in the AVO28 samples. All data have been corrected for mass bias, blank and other interferences by the reporting institution. Values for natural Si are from IUPAC [24].

Sample	$^{29}\text{Si}/^{30}\text{Si}$	$x(^{28}\text{Si})$	$x(^{29}\text{Si})$	$x(^{30}\text{Si})$	M_{VE}
NIST-5B2 P1	40.50	0.999 957 692(82)	$4.1289(81) \times 10^{-5}$	$1.020(9) \times 10^{-6}$	29.000 527
NIST-8A4 P1	40.26	0.999 957 741(80)	$4.1235(79) \times 10^{-5}$	$1.024(8) \times 10^{-6}$	29.001 667
NIST-5B1 P2 _{AVG}	37.00	0.999 957 503(78)	$4.1379(79) \times 10^{-5}$	$1.118(21) \times 10^{-6}$	29.002 739
NIST-8B1 P2 _{AVG}	36.85	0.999 957 876(61)	$4.1011(60) \times 10^{-5}$	$1.113(8) \times 10^{-6}$	29.002 844
NMIJ	34.92	0.999 9576	4.12×10^{-5}	1.18×10^{-6}	29.004 262
PTB	31.94	0.999 9575	4.12×10^{-5}	1.29×10^{-6}	29.006 772
PTB	34.38	0.999 9573	4.16×10^{-5}	1.21×10^{-6}	29.004 682
NRC	60.81	0.999 9588	4.05×10^{-5}	6.66×10^{-7}	28.992 629
Natural Si	1.52	0.922 23	0.046 85	0.030 92	

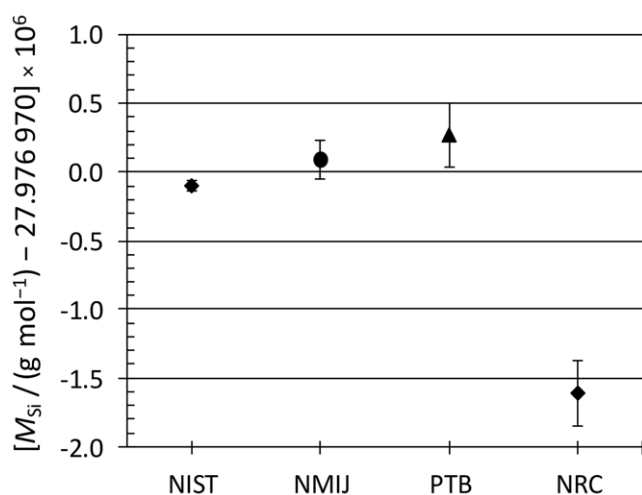


Figure 5. Comparison of the average absolute molar mass determinations of the AVO28 material by four different NMIs using the VE-IDMS technique. The values are differences at the 10^{-6} level between the measured molar masses and 27.976 970, as reported in this paper and by NMIJ [13], PTB [5] and NRC [12]. The uncertainties are combined standard uncertainties.

4. Discussion

Until this study, no measurable differences had been reported between the molar masses of chips sampled in the proximity of spheres S5 or S8. While the NIST results suggest the existence of a measurable difference in the molar mass of a sample from one of these two regions, this difference has been seen in only one sample (AVO28-5B1). This result, while singular, is supported by the following:

- (1) The much improved sensitivity of Si in the NIST experiments, which is largely a consequence of the simplified TMAH chemistry.
- (2) The maintenance of the same mass fraction of diluent (0.6% (mass fraction) TMAH) in all solutions, K -factor calibrants as well as the AVO28 and AVO28-IDMS samples.
- (3) The minimization of the range of Si mass fractions when going between K -factor, AVO28 and AVO28-IDMS samples. This was possible because of the first point in this

list. The most important consequence to limiting the range of Si mass fractions and holding the TMAH diluent mass fraction constant across all samples is that any variation in the mass bias experienced by the different solutions is minimized.

- (4) Always running the AVO28 samples as a pair (one from S5 and one from S8) that were corrected by a common K -factor and whose analysis order was randomized. This approach maximized the ability to detect any measurable differences between the different S5 and S8 samples.
- (5) The use of electronic switching of the Si isotope spectrum (via the dispersion lens), which allowed either Faraday or ion counting detection to be selected as the ^{30}Si signal intensity dictated. This was particularly important for measurements of the AVO28 and AVO28-IDMS samples and required no physical adjustments or changes to the instrument.
- (6) The use of a very high resolution slit ($16\ \mu\text{m}$) to increase the size of the ^{29}Si plateau in the presence of the ^{28}Si -hydride isobaric interference.
- (7) The use of a TMAH-H₂O cleaning solution prior to all blank and sample measurements. This cleaning step had two consequences. First, it minimized the impact of any memory carry-over arising from the isotopically different samples that needed to be run sequentially. By minimizing or eliminating memory, the abundances of any minor Si isotopes in a given sample could be measured with minimal memory bias without having to increase the Si mass fraction in the solution. It also allowed a stratified random sample run order to be used for data collection.
- (8) The use of two independently created K -factor solutions sets that confirmed the observed differences. This is a particularly rigorous check on the validity of the measurements, as it tests both the quality of the chemistry—from mass measurement to silicon dissolution to sample dilution—as well as the mass spectrometry.

The possible presence of a small but measurable variability in the molar mass of the AVO28 materials as well as the difference in the NRC molar mass determination and the NIST–NMIJ–PTB measurements are listed in table 9. This table compares the important $^{29}\text{Si}/^{30}\text{Si}$ ratios, amount-of-substance fractions

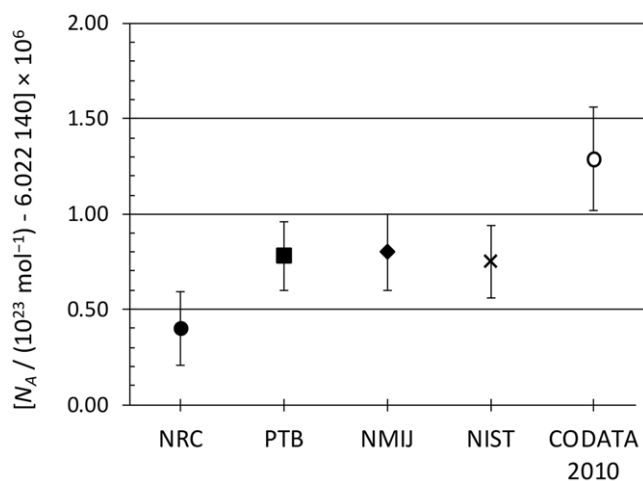


Figure 6. Comparison of the value of the Avogadro constant derived from the molar mass determinations of NRC [12], PTB [5], NMIJ [13] and NIST (this paper). The values for the Avogadro constants are the differences at the 10^{-6} level between the NMI-specific N_A and 6.022 140. The N_A values were either reported by the NMI (PTB, NRC) or were calculated using data on the density, mass and crystal lattice spacing for the two 1 kg silicon spheres [5] (NMIJ, NIST). Also shown is the current CODATA 2010 value for the Avogadro constant [10] which is a weighted average of IAC measurements and WB measurements. The uncertainty bars represent one standard uncertainty for the measurements.

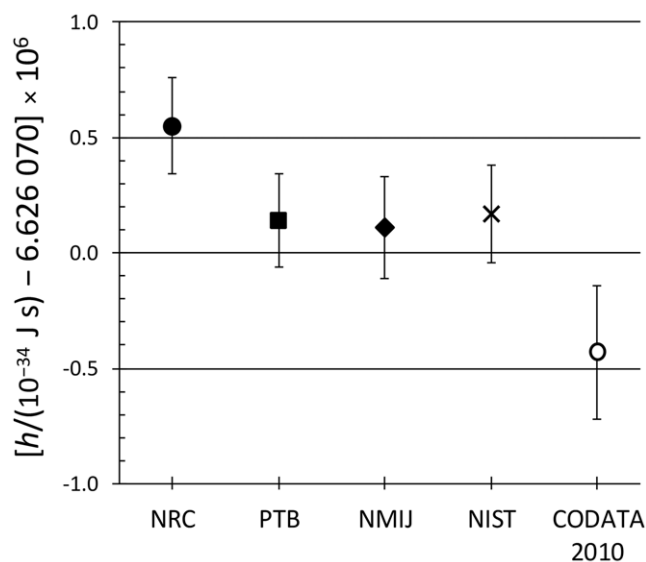


Figure 7. Comparison of the value of the Planck constant derived from the molar mass determinations of NRC [12], PTB [11], NMIJ [13] and NIST (this paper). The values for the Planck constants are the differences at the 10^{-6} level between the NMI-specific h and 6.626 070. The values were either reported by the NMI (PTB, NRC) or derived using the NMI-specific Avogadro constant (N_A) values and the molar Planck constant $N_A h$ [10] (NMIJ, NIST). Also shown is the current CODATA 2010 value for the Planck constant [10], which is a weighted average of IAC and WB measurements. The uncertainty bars represent one standard uncertainty for the measurements.

for the three Si isotopes in the AVO28 material and the fictive molar mass of the ‘virtual element’ (VE) as determined by the four NMIs.

Table 10. Summary of the Avogadro constants and Planck constants determined by the participating NMIs (NIST [this paper], NMIJ [13]; PTB [5] and NRC [12]). The uncertainties in parentheses are one standard uncertainty and apply to the last two significant digits.

NMI	Avogadro constant/mol ⁻¹	Planck constant/J s
NIST	6.022 140 76(19) × 10 ²³	6.626 070 17(21) × 10 ⁻³⁴
NMIJ	6.022 140 80(20) × 10 ²³	6.626 070 11(22) × 10 ⁻³⁴
PTB	6.022 140 78(18) × 10 ²³	6.626 070 14(20) × 10 ⁻³⁴
NRC	6.022 140 40(19) × 10 ²³	6.626 070 55(21) × 10 ⁻³⁴

As mentioned earlier, the principal cause of the difference in the NRC and NIST–NMIJ–PTB molar mass results appears to centre around the $x(^{30}\text{Si})$ values of AVO28, with the NRC reporting a ^{30}Si amount-of-substance fraction that is two times lower than that reported by NIST, NMIJ or PTB [23] (table 8). It is noteworthy however, that the amount-of-substance fractions of ^{28}Si determined by all three NMIs are quite similar (average $x(^{28}\text{Si}) = 0.999\,958$). The four different AVO28-IDMS measurements therefore gave essentially the same assay of the VE impurity, suggesting that the different calibration factors and AVO28-IDMS measurements are not only consistent but also correct despite the differences in the instrumental and chemistry procedures.

It is unlikely that the very large difference seen between the NRC and NIST–NMIJ–PTB absolute molar mass determinations reflects a real isotopic variability within the AVO28 material. More than a dozen samples from the AVO28 silicon boule have by now been carefully analysed for their absolute isotopic composition, and this study was the first to report a measurable difference between the silicon chips from the regions around spheres S5 and S8. This difference, moreover, has been seen in only one sample and was small ($\approx 4 \times 10^{-7} \text{ g mol}^{-1}$). The difference between the NIST–NMIJ–PTB and NRC molar mass results are, on the other hand, more than an order of magnitude larger ($\approx 2 \times 10^{-6} \text{ g mol}^{-1}$).

The last column of table 9 lists the calculated molar mass of the fictive VE-impurity (M_{VE}) for the different samples. While the NIST, NMIJ and PTB values overlap, the NRC value is lower, again reflecting their very low $x(^{30}\text{Si})$ amount-of-substance value. Thus, the key to the differences in the three absolute molar mass determinations is contained in the measurement and correction of the $^{29}\text{Si}/^{30}\text{Si}$ ratio of the AVO28 material. An explanation that the PTB and, by extension, the NIST and NMIJ values have been contaminated by natural silicon and are therefore lower has been put forward [12, 23], but additional studies and analyses have failed to confirm this.

PTB recently published a study [24] of Na-induced broadband interferences biasing the $^{29}\text{Si}/^{30}\text{Si}$ ratio. Specifically, scattered Na ions from the NaOH matrix can cause an anomalous increase in the ^{30}Si signal due to baseline issues. While the $x(^{29}\text{Si})$ amount-of-substance value they report [16] is identical to the NIST values, their $x(^{30}\text{Si})$ amount-of-substance value is somewhat higher, decreasing their $^{29}\text{Si}/^{30}\text{Si}$ ratio to 32. A correction of their ^{30}Si signal for the Na-induced broadband interference would increase their $^{29}\text{Si}/^{30}\text{Si}$ ratio towards the NIST value, supporting the proposition that a value near 39 is more representative of the AVO28 material instead of 60 as

suggested by the NRC [12]. Moreover, the NMIJ study combined the NIST TMAH chemistry with the NRC chemometric measurement approach and their molar mass as well as the AVO28 amount-of-substance fractions agree remarkably well with the NIST and PTB results. A closer examination of the systematic differences between these four different determinations is underway and will be reported when there is a better understanding of the controlling factors that have affected these measurements.

Finally, table 9 also gives some insight into the possible origin of the small molar mass difference observed in AVO28-5B1 P2 NIST sample. All four samples reported in this study have similar $^{29}\text{Si}/^{30}\text{Si}$ ratios, averaging 38.7. However, while the $x(^{28}\text{Si})$, $x(^{29}\text{Si})$ and $x(^{30}\text{Si})$ amount-of-substance values for samples 5B2 P1, 8A4 P1 and 8B1 P2 are very similar, 5B1 P2 has the lowest $x(^{28}\text{Si})$ amount-of-substance value. This suggests that the principal source of the observed variability is tied to a simple decrease in the amount of ^{28}Si , the dominant Si isotope ‘diluent’ in the AVO28 materials. The ^{29}Si and ^{30}Si abundances therefore increase slightly while remaining proportionate to the other AVO28 samples in terms of their amount-of-substance ratio.

5. Conclusions

NIST has produced calibrated molar mass measurements on four new samples from the IAC AVO28 ^{28}Si -enriched single crystal. The VE-IDMS approach developed by the PTB was used; however, by changing the Si chemistry and significantly modifying the mass spectrometry procedures, the combined standard uncertainty of the measured molar masses was reduced by at least a factor of two when compared with the previously reported measurements by PTB, NRC and NMIJ. By running pairs of samples and reducing the overall uncertainty of the measurement, a small but measurable isotopic difference in one of the AVO28 samples was detected when compared with the molar mass measurements of the three other samples. The data suggest that this variability could be controlled by small differences in the amount of ^{28}Si present within the different samples as the $^{29}\text{Si}/^{30}\text{Si}$ isotopic ratio remains relatively constant (≈ 38).

While the results from PTB, NRC and NMIJ molar mass determinations reported no measurable isotopic heterogeneities within their sample sets, a significant difference was noted between the NRC and PTB-NMIJ calculated molar masses for the AVO28 silicon. The results of this study agree with the PTB and NMIJ molar mass determinations and suggest that the actual AVO28 $^{29}\text{Si}/^{30}\text{Si}$ ratio is closer to 38 instead of 60 as reported by NRC. The derived values for the Avogadro constant ($N_{\text{A}} = 6.022\,140\,76(19) \times 10^{23} \text{ mol}^{-1}$) and the Planck constant ($h = 6.626\,070\,17(21) \times 10^{-34} \text{ J s}$) from the NIST measurements also agree with the values reported by PTB and NMIJ, within their stated uncertainties.

An online supplementary data file is available from stacks.iop.org/MET/51/361/mmedia that contains the raw and reduced data reported in this paper along with a detailed list of the data reduction equations. The latter are taken from [14, 21].

Acknowledgments

We would like to acknowledge the help and expertise of Vincent Lee, Patrick Abbott and Zeina Kubarych of the Mass and Force Group of the NIST Physical Measurement Laboratory (PML) for mass measurements and David Duerwer of the Chemical Sciences Division of the NIST Material Measurement Laboratory (MML) for automating the data transfer interface between instrument and offline computers. The suggestion by Lary Ball to use the smaller slit for greater resolution is gratefully acknowledged. Furthermore, the careful reviews and substantive suggestions made by David Duerwer (NIST-MML) and Barry Taylor (NIST-PML) helped focus and clarify the message of this research. Finally, all the support as well as the willing and open exchange of scientific ideas, information, samples and data reduction routines made available to us by our colleagues Axel Pramann, Olaf Rienitz and Detlef Schiel at the PTB were truly invaluable and are also gratefully acknowledged.

References

- [1] Mills I M, Mohr P J, Quinn T J, Taylor B N and Williams E R 2011 Adapting the International System of Units to the twenty-first century *Phil. Trans. R. Soc. A* **369** 3907–24
- [2] BIPM 2011 Resolution 1 ‘On the possible future revision of the International System of Units’ *24th General Conf. on Weights and Measures 2011* Available from: www.bipm.org/utis/common/pdf/24_CGPM_Resolutions.pdf
- [3] Stock M 2013 Watt balance experiments for the determination of the Planck constant and the redefinition of the kilogram *Metrologia* **50** R1–16
- [4] Li S S, Han B, Li Z K and Lan J 2012 Precisely measuring the Planck constant by electromechanical balances *Measurement* **45** 1–13
- [5] Andreas B et al 2011 Counting the atoms in a (^{28}Si) crystal for a new kilogram definition *Metrologia* **48** S1–13
- [6] Becker P, Pohl H J, Riemann H and Abrosimov N 2010 Enrichment of silicon for a better kilogram *Phys. Status Solidi a* **207** 49–66
- [7] Wang M, Audi G, Wapstra A H, Kondev F G, MacCormick M, Xu X and Pfeiffer B 2012 The AME2012 atomic mass evaluation: II. Tables, graphs and references *Chin. Phys. C* **36** 1603–2014
- [8] Becker P 2005 High precision measurement of the Avogadro constant based on silicon *AIP Conf. Proc.* **772** 69–72
- [9] Mohr P J, Taylor B N and Newell D B 2012 CODATA Recommended values of the fundamental physical constants: 2010 *J. Phys. Chem. Ref. Data* **41** 043109
- [10] Mohr P J, Taylor B N and Newell D B 2012 CODATA recommended values of the fundamental physical constants: 2010 *Rev. Mod. Phys.* **84** 1527–605
- [11] Pramann A, Rienitz O, Schiel D, Schlote J, Guttler B and Valkiers S 2011 Molar mass of silicon highly enriched in ^{28}Si determined by IDMS *Metrologia* **48** S20–5
- [12] Yang L, Mester Z, Sturgeon R E and Meija J 2012 Determination of the atomic weight of ^{28}Si -enriched silicon for a revised estimate of the Avogadro constant *Anal. Chem.* **84** 2321–7
- [13] Narukawa T, Hioki A, Kuramoto N and Fujii K 2014 Molar mass measurement of a ^{28}Si -enriched silicon crystal for determination of the Avogadro constant *Metrologia* **51** 161–8
- [14] Rienitz O, Pramann A and Schiel D 2010 Novel concept for the mass spectrometric determination of absolute isotopic

- abundances with improved measurement uncertainty: I. Theoretical derivation and feasibility study *Int. J. Mass Spectrom.* **289** 47–53
- [15] Pramann A, Rienitz O, Schiel D and Guttler B 2011 Novel concept for the mass spectrometric determination of absolute isotopic abundances with improved measurement uncertainty: II. Development of an experimental procedure for the determination of the molar mass of silicon using MC-ICP-MS *Int. J. Mass Spectrom.* **299** 78–86
- [16] Pramann A, Rienitz O, Schiel D, Guttler B and Valkiers S 2011 Novel concept for the mass spectrometric determination of absolute isotopic abundances with improved measurement uncertainty: III. Molar mass of silicon highly enriched in ^{28}Si *Int. J. Mass Spectrom.* **305** 58–68
- [17] Bulska E, Drozdov M N, Mana G, Pramann A, Rienitz O, Sennikov P and Valkiers S 2011 The isotopic composition of enriched Si: a data analysis *Metrologia* **48** S32–6
- [18] Drozdov M, Drozdov Y, Pryakhin D, Shashkin V, Sennikov P and Pohl H J 2010 Qualitative SIMS analysis of $^{28,29,30}\text{Si}$ isotope concentration in silicon using a TOF.Sims-5 Setup *Bull. Russ. Acad. Sci.: Phys.* **74** 75–7
- [19] Andreas B et al 2011 Determination of the Avogadro constant by counting the atoms in a ^{28}Si crystal *Phys. Rev. Lett.* **106** 030801
- [20] JCEM 2012 *International Vocabulary of Metrology—Basic and General Concepts and Associated Terms* (VIM) [database on the Internet] JCGM 200. Available from: www.bipm.org/utis/common/documents/jcgm/JCGM_200_2012.pdf
- [21] Mana G and Rienitz O 2010 The calibration of Si isotope ratio measurements *Int. J. Mass Spectrom.* **291** 55–60
- [22] Kessel R 2012 GUM Workbench Pro Version 2.4.1.402 ed Im Winkel 15-1, D-79576, Weil am Rhein, Germany: Metrodata GmbH
- [23] Steele A G, Meija J, Sanchez C A, Yang L, Wood B M, Sturgeon R E, Mester Z and Inglis A D 2012 Reconciling Planck constant determinations via watt balance and enriched-silicon measurements at NRC Canada *Metrologia* **49** L8–10
- [24] Pramann A, Rienitz O and Schiel D 2012 Silicon isotope ratios affected by sodium-induced broadband interference in high resolution multicollector-ICPMS *Anal. Chem.* **84** 10175–9
- [25] Berglund M and Wieser M E 2011 Isotopic compositions of the elements 2009 (IUPAC Technical Report) *Pure Appl. Chem.* **83** 397–410